Proposal for Generating Brilliant X-Ray Beams Carrying Orbital Angular Momentum

Shigemi Sasaki and Ian McNulty
Advanced Photon Source, Argonne National Laboratory, 9700 South Cass Avenue, Argonne, Illinois 60439, USA
(Received 9 September 2007; published 24 March 2008)

We consider use of a variable polarizing undulator for generating brilliant x-ray beams carrying orbital angular momentum. We find that higher harmonics of the radiation correspond to Laguerre-Gaussian modes with azimuthal mode indices l equal to one less than the harmonic number when the undulator is operated to produce circularly polarized light. Beams with nonzero l carry orbital angular momentum quantized in units of $l\hbar$ per photon. When operated to produce linear polarization, the harmonics correspond to Hermite-Gaussian modes. Selection of these modes with conventional monochromator optics opens the door for new research with x-ray synchrotron and free-electron laser sources.

DOI: 10.1103/PhysRevLett.100.124801 PACS numbers: 41.50.+h, 07.85.Fv, 41.60.Ap, 41.60.Cr

Phase singularities and photon beams that carry orbital angular momentum (OAM) are of great interest to the optics and laser communities for applications ranging from manipulation of small particles and Bose-Einstein condensates to quantum entanglement and radio astronomy [1–7]. These remarkable properties of photons were recently demonstrated in the x-ray regime [8,9] and may be useful to probe weak quadrupolar and higher-order transitions in matter [10,11]. However, in comparison to the radio and visible light regimes, it is difficult to fabricate efficient achromatic optics to produce x-ray beams with phase singularities. In addition to this inconvenience, there has been no investigation of the possibility of using a synchrotron source to generate a singular x-ray beam directly. As is well known, a linear undulator does not generate even harmonics on axis and a helical undulator does not generate any harmonics (except the fundamental) on axis. As a result, the off-axis higher harmonic radiation, especially the even harmonics, have been considered useless, and its properties have not been investigated intensively.

Last year, a group working on the VISA (Visible to Infrared SASE Amplifier) free-electron laser experiment at Brookhaven National Laboratory observed donut-shaped and spiral intensity distributions of the infrared radiation [12,13], indicating the possible existence of OAM states. Recently, we showed preliminary evidence that the second-harmonic radiation from a helical undulator carries OAM [14,15]. In this Letter we show that all the harmonics except the fundamental from a variable polarizing undulator such as an Advanced Planar Polarized Light Emitter (APPLE) device [16] are described by Laguerre-Gaussian (LG) modes carrying OAM, when it is phased to deliver circularly polarized radiation. Planar undulators and APPLE devices phased to deliver linearly polarized radiation produce harmonics described by Hermite-Gaussian (HG) modes, which do not carry OAM.

The photon beam intensity radiated per unit frequency and unit solid angle from an accelerated relativistic electron is given by [17]

$$\frac{d^2I}{d\omega d\Omega} = \frac{e^2\omega^2}{16\pi^3\varepsilon_0 c}\left|\int_{-\infty}^{\infty}\{\vec{n}\times(\vec{n}\times\vec{\beta})\}e^{i\omega(t-n\cdot r/c)}dt\right|^2, \tag{1}$$

where $\vec{n}$ is the unit vector and $\vec{\beta}$ is the relativistic velocity vector. Starting from this equation, we can derive more practical equations by assuming the magnetic field and hence the electron trajectory is periodic. In any operational mode (linear, elliptical, or circular) of an APPLE undulator, the phase difference between the horizontal and the vertical components of the periodic magnetic field is $\pi/2$; hence, the axis of the polarization ellipse stays in the horizontal plane. In this case the intensity is given by [18]

$$\frac{d^2I}{d\omega d\Omega} = \frac{e^2\gamma^2 n^2\xi^2}{4\pi\varepsilon_0 c}[|A_x|^2 + |A_y|^2]L(N\Delta\omega/\omega_1), \tag{2}$$

where the horizontal and vertical components A_x and A_y of the nth harmonic amplitude are given by

$$\begin{aligned} &A_x = 2\gamma\theta\cos\phi S_0 - K_y(S_1 + S_{-1}) \\ \text{and}\quad &A_y = 2\gamma\theta\sin\phi S_0 + iK_x(S_1 - S_{-1}), \end{aligned} \tag{3}$$

and where

$$S_q = \sum_{p=-\infty}^{\infty} J_p(Y)J_{n+2p+q}(X)e^{i(n+2p+q)\Phi},$$

and

$$\begin{aligned} &X = 2n\xi\gamma\theta\sqrt{K_y^2\cos^2\phi + K_x^2\sin^2\phi}, \\ &Y = n\xi(K_y^2 - K_x^2)/4, \tan\Phi = (K_x/K_y)\tan\phi, \\ \text{and}\quad &\xi = 1/(1 + \gamma^2\theta^2 + K_x^2/2 + K_y^2/2). \end{aligned}$$

Here, $L(N\Delta\omega/\omega_1)$ is the one-dimensional Laue function for the number of periods N, ω_1 is the angular frequency of the fundamental radiation; $\Delta\omega = \omega - n\omega_1(\theta)$; θ is the observation angle from the radiation axis; ϕ is the azimuthal angle in the x-y plane at the observer's position; γ is the Lorentz factor of the electrons traversing the

TABLE I. Dependence of the second-harmonic electric field amplitude on the azimuthal angle.

ϕ	A_x	A_y	A
0	$(2\gamma\theta - 4K/X)J_2(X)$	$-2iKJ_2{}'(X)$	$\sqrt{2}\{(\gamma\theta - 2K/X)J_2(X) - KJ_2{}'(X)\}$
$\pi/2$	$-2iKJ_2{}'(X)$	$-(2\gamma\theta - 4K/X)J_2(X)$	$i\sqrt{2}\{(\gamma\theta - 2K/X)J_2(X) - KJ_2{}'(X)\}$
π	$-(2\gamma\theta - 4K/X)J_2(X)$	$2iKJ_2{}'(X)$	$-\sqrt{2}\{(\gamma\theta - 2K/X)J_2(X) - KJ_2{}'(X)\}$
$3\pi/2$	$2iKJ_2{}'(X)$	$(2\gamma\theta - 4K/X)J_2(X)$	$-i\sqrt{2}\{(\gamma\theta - 2K/X)J_2(X) - KJ_2{}'(X)\}$

device; K is the undulator magnetic deflection parameter, $q = -1, 0, 1$; and J_n is the nth order Bessel function of the first kind.

For the pure circular case, $K_y = K_x = K$, $X = 2n\xi\gamma\theta K$, $Y = 0$, and $\Phi = \phi$. After simple manipulation, we obtain

$$A_x = e^{in\phi}\{2\gamma\theta\cos\phi J_n(X) - K(J_{n+1}(X)e^{i\phi} + J_{n-1}(X)e^{-i\phi})\}$$

and
$$A_y = e^{in\phi}\{2\gamma\theta\sin\phi J_n(X) + iK(J_{n+1}(X)e^{i\phi} - J_{n-1}(X)e^{-i\phi})\}. \quad (4)$$

For the linear case, $K_x = 0$ and $\Phi = 0$, and we have

$$A_x = 2\gamma\theta\cos\phi S_0 - \frac{1}{\xi\gamma\theta\cos\phi}\left(S_0 + \frac{2}{n}S_2\right) \quad (5)$$

and
$$A_y = 2\gamma\theta\sin\phi S_0,$$

where

$$S_2 = \sum_{p=-\infty}^{\infty} pJ_p(Y)J_{n+2p}(X).$$

Equations (4) and (5) are valid for all harmonics of the radiation for the circular and linear cases, respectively.

The total intensity is obtained by summing the squared magnitudes of the horizontal and vertical components $|A_x|^2$ and $|A_y|^2$. Table I shows the relation between the ϕ and the phase of the electric field amplitude for the second harmonic. It is clear that the sign of each component reverses with each half-turn around the propagation axis; thus, the phase of the radiation tracks the azimuthal angle. Figure 1 shows the angular distribution of the intensity calculated with Eq. (4) for the second, third, and fourth harmonics for the circular mode and $K = 1$, for a single electron. The distributions have azimuthal symmetry and resemble the characteristic "optical donut" shape associated with LG beams [2]. However, this shape alone does not necessarily mean the radiation carries OAM.

To explore whether the harmonics carry OAM in general, we consider the time-independent complex amplitude. For the circular case this can be written as

$$A = (A_x - iA_y)/\sqrt{2} = \sqrt{2}e^{i(n-1)\phi}\{\gamma\theta J_n(X) - KJ_{n-1}(X)\}$$
$$= \sqrt{2}e^{i(n-1)\phi}\left\{\left(\gamma\theta - \frac{nK}{X}\right)J_n(X) - KJ_n{}'(X)\right\}, \quad (6)$$

where $J_n{}'$ is the first derivative of J_n with respect to X. Since the bracketed terms have no azimuthal dependence, we see that Eq. (6) is a special case of an LG mode with an azimuthal mode index or topological charge of $l = n - 1$. LG beams carry OAM quantized in units of $l\hbar$ per photon [1]. Figure 2 shows the angular distribution of the first, second, third, and fourth harmonic intensity, magnitude, and phase calculated with Eq. (6). As one can observe from the phase patterns, the second and higher harmonics describe phase singularities with $l = 1, 2, 3$, and so on. The phase information can also be retrieved by Fourier decomposition of the time-dependent field obtained by Eq. (1). For the second harmonic, for example, the peak amplitude shifts by $\lambda/4$ for each $\pi/2$ rotation of ϕ [14]. This helical phase signature is again evidence that the second harmonic carries OAM with an azimuthal mode index of $l = 1$.

In contrast to the radiation from a circular device, the radiation emitted by a planar undulator or an APPLE device phased to deliver linearly polarized light is described by HG modes, which are equivalent to certain low-order transverse electric-magnetic modes (TEM_{01}, TEM_{02}, ...). These modes do not carry OAM; however, they can be converted to LG modes with cylindrical lenses. Figure 3 shows the angular intensity distributions of the σ component (horizontal linear polarization) of the first few harmonics calculated by Eq. (5) for $K = 1$. The intensity distributions of the second and third harmonics (Fig. 4) are in good agreement with earlier studies [19]. By putting $n = 2$ and $\phi = 0, \pi$ in Eq. (3) and using the fact that $S_0(X) = S_0(-X)$ and $S_2(X) = S_2(-X)$ for even values of n, we get

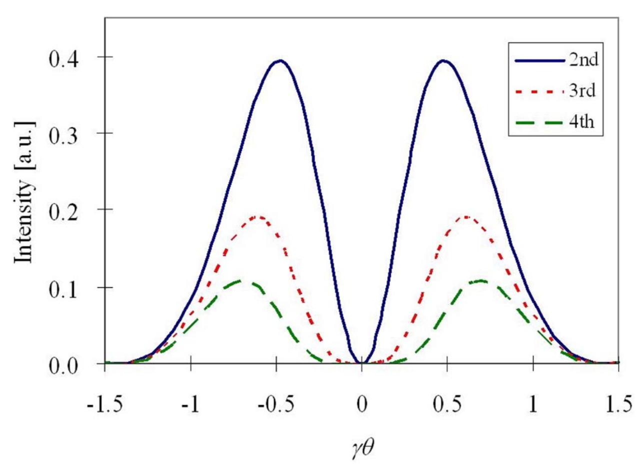

FIG. 1 (color online). Single-electron angular intensity distributions of second (solid line), third (dashed line), and fourth (broken line) harmonics for a circular undulator and $K = 1$.

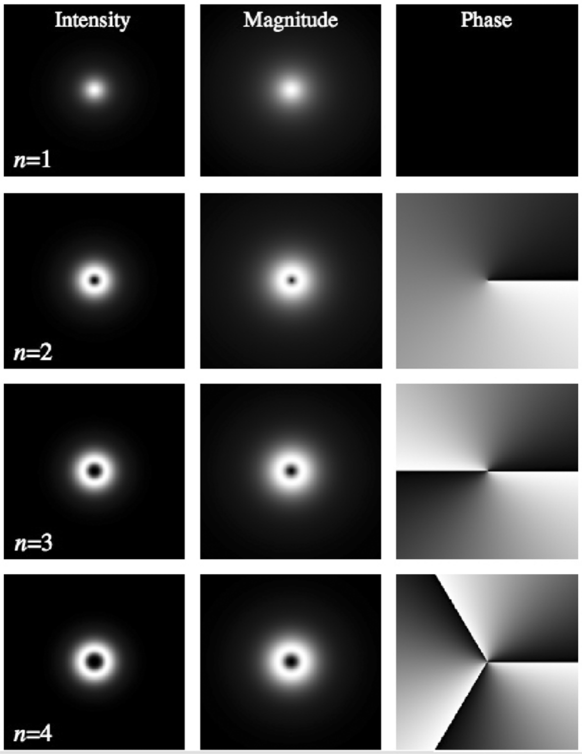

FIG. 2. Calculated intensity, magnitude, and phase of the first, second, third, and fourth harmonics in the $(\gamma\theta, \phi)$ plane. The intensity and magnitude of A are shown on the same gray scales for comparison. The phase $\Phi = \tan^{-1}\{\mathrm{Im}(A)/\mathrm{Re}(A)\}$ is represented as a gray scale. Black and white are relative phase angles of 0 and 2π radians, respectively.

$$A_x(\phi = \pi) = -A_x(\phi = 0).$$

We see that the radiation amplitude is 180° out of phase at $\phi = 0$ and $\phi = \pi$, corresponding to an HG mode with $l = 1$ and which is equivalent to the TEM_{01} mode.

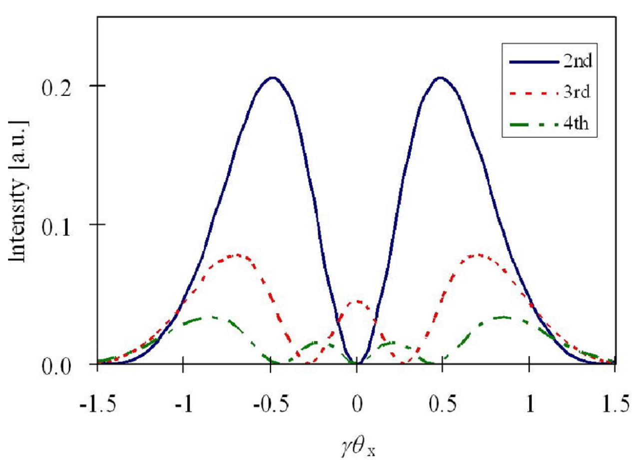

FIG. 3 (color online). Angular intensity distributions of the second (solid line), third (dashed line), and fourth (broken line) harmonics of a linear undulator. The deflection parameter K equals one.

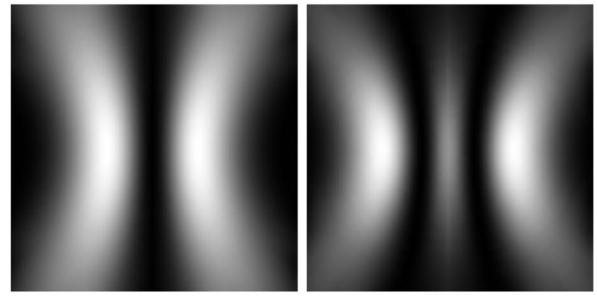

FIG. 4. Radiated intensity distributions of the σ component of the second and third harmonics in the $(\gamma\theta, \phi)$ plane for the linear device and $K = 1$.

In the discussion above, we only considered radiation from a single electron in order to clarify its intrinsic mode properties. In actuality, the electron beam passing through an undulator has a finite spatial and angular distribution. The effect of the finite electron beam dimensions is well approximated by convolving the single-electron radiation amplitude from Eq. (1) with a Gaussian function representing the electron beam profile. A realistic simulation of the radiated intensity from an actual synchrotron source is straightforward to obtain numerically. Figure 5 shows the calculated intensity distribution using the code SPECTRA [20] of the second harmonic from the circularly polarizing undulator (CPU) installed in the Advanced Photon Source (APS) storage ring [21].

For this computation, we used the current APS beam parameters (7-GeV beam energy, 2.5-nm-rad horizontal emittance, and 0.1% coupling) and the actual magnetic field data at the maximum field strength (K parameter of approximately 2.77) of the 128-mm-period CPU. The photon beam intensity in the bright annular ring exceeds 10^{12} photons/s/mm^2/0.1% BW at 50 m from the undulator, for a stored electron beam current of 100 mA. The

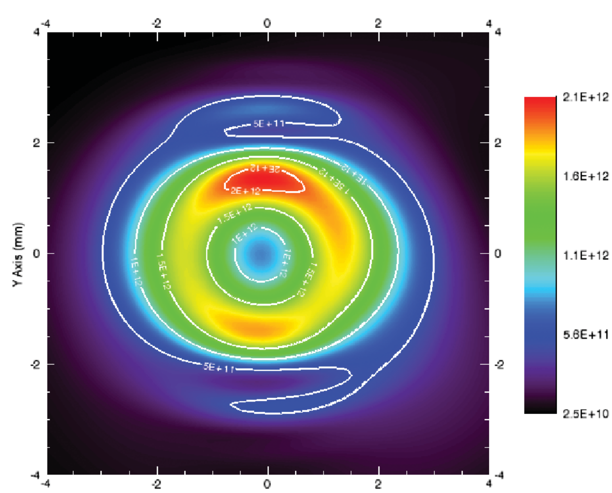

FIG. 5 (color). Calculated intensity distribution of the second harmonic from the APS CPU for $K = 2.77$, a photon energy of 830 eV, at a distance of 50 m.

nonvanishing intensity on axis arises from incoherent superposition of the many coherent modes present in the beam, especially in the horizontal plane due to the large source size. The upper region of the annulus is brighter because the electron beam makes an additional half-turn above the symmetry axis due to the magnetic structure of the CPU. The vortical nature of the beam is also evident in the weak outer lobes, which can be explained by redshifted off-axis contributions from the third and higher harmonics.

Direct production of high brilliance LG and HG beams offers several advantages. First, optical components such as refractive phase plates and holographic gratings are unnecessary to generate these transverse modes. Second, the x-ray beam energy is easily tuned by changing the strength of the undulator magnetic field on the electron beam axis (typically by adjusting the gap between the field poles). Third, for LG beams the azimuthal mode can be chosen with a monochromator, and the OAM helicity can be reversed by shifting the phase of the magnetic field by 180° in circular operation. The contribution of undesired azimuthal modes at large angles can be mitigated by use of an aperture. In addition, the first-harmonic ($l = 0$) radiation can be suppressed by installing a second undulator following the first with a suitable phase delay between them.

Much as the advent of polarized x-ray sources has dramatically expanded our understanding of magnetism, we anticipate that the availability of intense x-ray beams carrying orbital in addition to spin angular momentum will open the door to new condensed matter research via x-ray scattering and spectroscopy methods [11]. These previously unappreciated properties of undulator radiation may also prove useful for x-ray spiral phase contrast microscopy of biological specimens [22] and for structural determination of light-atom chiral molecules such as proteins and pharmaceuticals by x-ray diffraction in the absence of anomalous dispersion [23]. Furthermore, the intensity and purity of these singular x-ray modes will be tremendously enhanced using energy recovery linac and free-electron laser sources [24], potentially leading to novel x-ray quantum optics experiments in the femtosecond regime. Finally, we note that a superconducting helical undulator installed in the 150-GeV electron linac of the proposed International Linear Collider has the capability to generate gamma rays carrying OAM for nuclear and particle physics [25].

We thank E. Gluskin, C. Quitmann, and M. Padgett for insightful comments on this subject. One of the authors (S. S.) thanks T. Shimada at JAEA for stimulating his interest to investigate the properties of undulator radiation. This work was supported by the U.S. Department of Energy, Office of Science, Office of Basic Energy Sciences, under Contract No. DE-AC02-06CH11357.

[1] L. Allen, M. W. Beijersbergen, R. J. C. Spreeuw, and J. P. Woerdman, Phys. Rev. A **45**, 8185 (1992).
[2] M. Padgett, J. Courtial, and L. Allen, Phys. Today **57**, No. 5, 35 (2004).
[3] J. Leach, M. J. Padgett, S. M. Barnett, S. Franke-Arnold, and J. Courtial, Phys. Rev. Lett. **88**, 257901 (2002).
[4] D. G. Grier, Nature (London) **424**, 810 (2003).
[5] A. Mair, A. Vaziri, G. Weihs, and A. Zeilinger, Nature (London) **412**, 313 (2001).
[6] M. F. Andersen, C. Ryu, P. Cladé, V. Natarajan, A. Vaziri, K. Helmerson, and W. D. Phillips, Phys. Rev. Lett. **97**, 170406 (2006).
[7] B. Thidé, H. Then, J. Sjöholm, K. Palmer, J. Bergman, T. D. Carozzi, Ya. N. Istomin, N. H. Ibragimov, and R. Khamitova, Phys. Rev. Lett. **99**, 087701 (2007).
[8] A. G. Peele *et al.*, Opt. Lett. **27**, 1752 (2002).
[9] A. G. Peele, K. A. Nugent, A. P. Mancuso, D. Paterson, I. McNulty, and J. P. Hayes, J. Opt. Soc. Am. A **21**, 1575 (2004).
[10] A. Alexandrescu, D. Cojoc, and E. Di Fabrizio, Phys. Rev. Lett. **96**, 243001 (2006).
[11] M. VanVeenendaal and I. McNulty, Phys. Rev. Lett. **98**, 157401 (2007).
[12] G. Andonian *et al.*, in *Proceedings of the FEL 2006 Conference, Berlin, 2006* (BESSY, Berlin, 2006), p. 443; http://www.jacow.org.
[13] E. Hemsing *et al.*, in *Proceedings of the 2007 Particle Accelerator Conference* (IEEE, Albuquerque, NM, 2007), p. 1263; http://www.jacow.org.
[14] S. Sasaki, I. McNulty, and R. J. Dejus, in *Proceedings of the 14th National SRI Conference, Baton Rouge, LA* [Nucl. Instrum. Methods Phys. Res., Sect. A **582**, 43 (2007)].
[15] S. Sasaki, I. McNulty, and T. Shimada, in *Proceedings of the 2007 Particle Accelerator Conference* (IEEE, Albuquerque, NM, 2007), p. 1142; http://www.jacow.org.
[16] S. Sasaki, Nucl. Instrum. Methods Phys. Res., Sect. A **347**, 83 (1994).
[17] J. D. Jackson, *Classical Electrodynamics* (Wiley, New York, 1975), 2nd ed., p. 668.
[18] B. Kincaid, J. Appl. Phys. **48**, 2684 (1977); R. P. Walker, Proceedings of the 1997 CERN Accelerator School, CERN Report No. 98-04, p. 129.
[19] See, for example, *Undulators, Wigglers and Their Applications*, edited by H. Onuki and P. Elleaume (Taylor & Francis, New York, 2003), p. 87.
[20] T. Tanaka and H. Kitamura, J. Synchrotron Radiat. **8**, 1221 (2001).
[21] E. Gluskin *et al.*, AIP Conf. Proc. **521**, 344 (2000).
[22] A. Jesacher, S. Fürhapter, S. Bernet, and M. Ritsch-Marte, Phys. Rev. Lett. **94**, 233902 (2005).
[23] R. Raval, Nature (London) **425**, 463 (2003).
[24] For example, see: D. Bilderback *et al.*, J. Synchrotron Radiat. **10**, 346 (2003); http://xfel.desy.de/; and http://www.elettra.trieste.it/FERMI/.
[25] Documentation on the ILC project can be found at http://www.linearcollider.org/cms/.